Extensive linear ridge networks in Nili Fossae and Nilosyrtis, Mars: implications for fluid flow in the ancient crust

Lee Saper[1] and John F. Mustard[1]

Received 25 October 2012; revised 14 December 2012; accepted 18 December 2012; published 30 January 2013.

[1] We have undertaken high-resolution mapping of the distribution, physical characteristics, orientation, and stratigraphic occurrence of >4000 linear ridge segments in two study areas, the Nilosyrtis highlands and the Nili Fossae region covering $1 \times 10^5\,km^2$. Ridges are typically hundreds of meters in length, meters in width, and up to tens of meters in height. Ridges form intersecting networks of anastomosing and bifurcating segments and consequently have variable orientations. Ridges are expressed in altered and brecciated basement materials on the floors and rims of impact craters deeply eroded by fluvial and other processes. The ridge-bearing basement is the lowest exposed stratigraphic unit and is overlain by a relatively unaltered mafic cap rock. Ridges are observed to terminate at the contact of these two units. We interpret the ridges to represent a complex of fractures, faults, shear zones, clastic and melt-bearing dikes, and pseudotachylytes that have been variably indurated by fluid percolation and mineralization. The fluid conduits were hardened relative to the host rock and are expressed as ridges due to differential erosion. The orientations of the exhumed ridges record the state of stress in the crust at the time of formation. In Nili Fossae, a significant population of ridges is aligned with the orientations of the Nili Fossae graben, indicating that their emplacement may be related to crustal loading of the Isidis Basin after the impact event. The association of ridges with the hydrated mineral-bearing basement suggests that, in the postimpact environment, the fractures served as conduits of preferential fluid flow, which were cemented by mineral precipitation. **Citation:** Saper, L., and J. F. Mustard (2013), Extensive linear ridge networks in Nili Fossae and Nilosyrtis, Mars: implications for fluid flow in the ancient crust, *Geophys. Res. Lett.*, *40*, 245–249, doi:10.1002/grl.50106.

1. Introduction

[2] Based on the composition and stratigraphy of phyllosilicates exposed on Mars, *Ehlmann et al.* [2011] suggested that subsurface hydrologic processes were key drivers of alteration of the early Martian crust; however, the study failed to address evidence of physical mechanisms for fluid transport through a permeable crust. On sol 2769 of its mission, Mars Exploration Rover Opportunity encountered a gypsum vein cutting through Noachian-aged materials exhumed at Endeavor Crater, providing macroscopic evidence of low-temperature fluids percolating through and mineralizing fractures in rock [*Squyres et al.*, 2012]. Similar veins appear to be commonly expressed in impact-disrupted materials at Endeavor Crater, but whether such features are pervasive in Noachian terrains elsewhere is unknown. The goal of this study is to begin the characterization of possible fossilized conduits for subsurface fluid flow preserved on Mars and to assess the implications for the geologic evolution and habitability of the planet.

[3] *Head and Mustard* [2006] proposed that networks of ridges observed in a few impact craters north of Syrtis Major represent the expression of breccia dikes that were preferentially hardened and exposed by differential erosion. Similar linear features expressed as topographic ridges are exposed in the clay-bearing brecciated basement in Nili Fossae and have been noted by numerous investigators [*Mangold et al.*, 2007; *Mustard et al.*, 2007, 2009; *Ehlmann et al.*, 2009; *Ivanov et al.*, 2012] but have not been studied in detail. The ridges have a spatial scale of meters in width and hundreds of meters in length and require high-resolution imagery to resolve their detailed physical characteristics and relationship to surrounding units. Hypotheses for the origin of these features, based on comparative morphology to similar ridges observed elsewhere on Mars, Earth, and the Moon, include exhumed igneous dikes, breccia dikes, fluid-cemented fractures, shear hardened fractures or deformation bands [*Okubo and McEwen*, 2007], exposed pseudotachylyte dikes, inverted fluvial channels, and eskers. All of these hypotheses (except eskers) invoke differential erosion to account for the positive topographic relief.

[4] With broad coverage of higher spatial resolution imagery from the Mars Reconnaissance Orbiter, we have undertaken a comprehensive analysis of ridge distribution, morphology, and orientation in the context of their stratigraphic relationship to other units to better constrain the hypotheses for the origin of the ridge networks. In the Nilosyrtis highlands, we follow up on lower-resolution mapping from *Head and Mustard* [2006] and assess their interpretations in light of new orbital spacecraft imagery, primarily the Context Imager (CTX; 6 m/pxl) and the High-Resolution Imaging Science Experiment (HiRISE; 0.25 m/pxl) [*Malin et al.*, 2007; *McEwen et al.*, 2007]. In Nili Fossae, we provide the first detailed descriptions and distribution mapping of exposed ridges. In both locations, we present new quantitative data on the strike orientations of ridge segments.

2. Methods

2.1. Regional Setting

[5] The Nilosyrtis region is defined as the highlands region north of the Syrtis Major volcanic complex and is

[1]Department of Geological Sciences, Brown University, Providence, Rhode Island, USA.

Corresponding author: L. Saper, Department of Geological Sciences, Brown University, Providence, Rhode Island, USA. (leesaper@gmail.com)

©2013. American Geophysical Union. All Rights Reserved.
0094-8276/13/10.1002/grl.50106

bound on the east by the northwestern rim of the Isidis Basin (centered at 85.7°E, 13°N [*Tornabene et al.*, 2008]). The Nili Fossae region lies within a segment of the preserved rim of the 1900-km diameter Isidis impact basin, is characterized by the large Isidis-concentric graben [*Wichman and Schultz*, 1989], and is superposed by Syrtis lavas to the south (Figure 1). Since the Viking era, this region has been recognized to preserve a diversity of geologic processes operating from the Noachian period through the Amazonian and has been studied for its complex interaction of impact basin formation, tectonic modification, volcanic resurfacing, fluvial activity, and intense denudation and mass removal processes. The region's complex history of geologic processes, some water-related, provides an excellent study area to understand the structure, composition, and dynamics of the early Martian crust due to its widespread exposure.

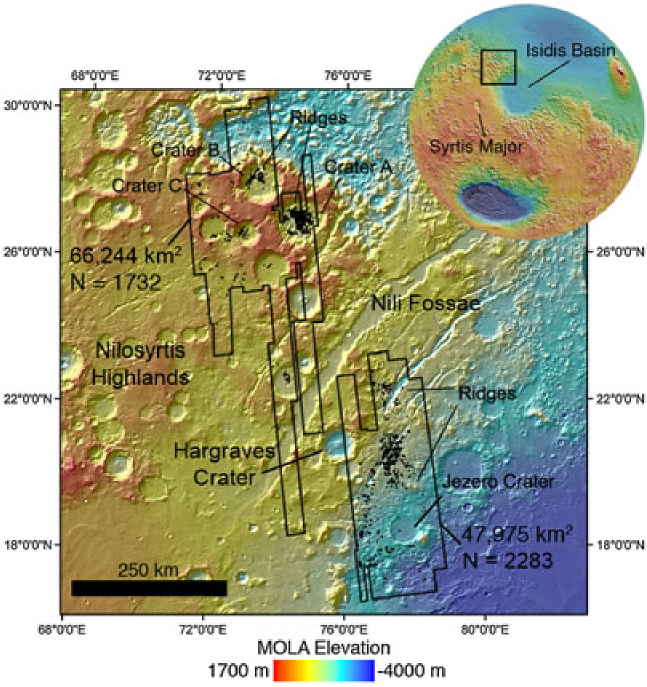

Figure 1. Mars Orbiter Laser Altimeter (MOLA) gridded elevation (-1700 to -4000 m) showing large-scale topography of study region. (black polygons) Two areas of detailed geologic mapping. (small black lines) Location of ridge networks and segments. (top right) MOLA image of the eastern hemisphere of Mars showing geographic context of study region. (black box) Approximate location of the top frame.

2.2. Mapping Criteria and Measurements

[6] Criteria were developed to differentiate ridges from other linear features to consistently map the same geologic feature and avoid including other morphologies in the analysis. Ridges were defined as sharply tapered linear to curvilinear features with large length-width aspect ratios that express topographic relief (Figure 2). The ridges often bifurcate and form interconnected networks of variably oriented ridges but can also exist as isolated landforms. Linear features that were excluded from the analysis include scarps, dunes, yardangs, wrinkle ridges associated with volcanic flows, troughs, and streamlined impact ejecta features. Some linear features were too small to resolve at CTX spatial resolution and were omitted unless they were clearly part of a developed array of ridges and could be resolved by HiRISE imagery. When two or more ridges overlapped, individual ridge segments were defined as features that were continuous along strike even when intersecting other ridges. Ridges that appeared to abruptly change direction were counted as two individual segments.

[7] Orientations were represented as a vector connecting individual ridge segment end points. The vector geographic orientations were computed as angles from 0° to 360°. Because the absolute orientation computed for each ridge depended on the choice of start and end points (i.e., 45° = 225°), orientations from 181° to 360° were rotated and binned to 0–180°. We computed length with the same start and end points used in the orientation analysis, approximating most ridges as straight lines. Ridge heights were estimated using digital elevation models (DEMs) made from CTX and HiRISE stereopairs (~6 and ~1 m/pxl, respectively) by measuring the difference in elevation relative to the geoid between a ridge crest and its immediate surroundings. Because the DEMs were not

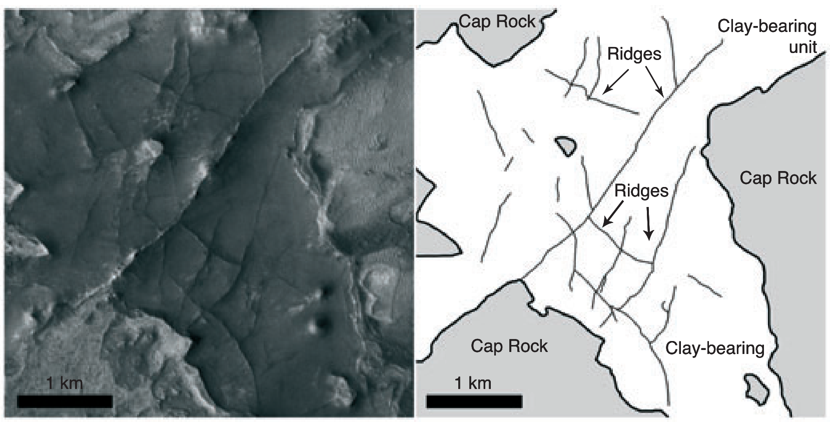

Figure 2. (left) Subframe of CTX P05_002888_2025_XI_22N283W showing type locality of ridge networks exposed in Nili Fossae. Ridges are narrow linear features that form branched networks. Low albedo unit that the ridges reside in is Fe/Mg smectite bearing. (right) Corresponding ArcGIS geologic map showing locations of ridge segments (thin lines).

registered to a calibrated elevation grid, absolute height and quantitative dip measurement were not considered. Examples of typical ridge exposures and high-resolution mapping are shown in Figure 2.

3. Results

3.1. Distribution and Physical Characteristics

[8] Using CTX images, we mapped the physical characteristics, morphology, strike orientation, and stratigraphic occurrence of >4000 linear ridge segments at ~1:25,000 scale in two mapping areas, a 66,244 km^2 region extending from 18–30°N and 71–75°E corresponding to the cratered Nilosyrtis highlands and a 47,975 km^2 region covering 16.5–23°N and 75.5–79°E corresponding to the Nili Fossae region (Figure 1). Ridge networks of variable scale and density are exposed in heavily eroded locales within the study areas and tend to be associated with impact craters, where the densest ridge populations occur. Our results indicate that elements of the gross morphology and spatial dimensions of ridge populations appear to be common to all mapping areas, with local variation in average ridge length, the shape of orientation distributions, and orientation frequency maxima (Figure 3). For the entire mapped population (n = 4020), the average ridge length is 533.7 m with a standard deviation of 510.9 m and 36 ridges over 3 km in length. A summary of ridge strike orientation data is shown in rose plot diagrams in Figure 3 plotted from 0° to 180°, with 0° and 180° representing geographic north and south, respectively. Three craters from the Nilosyrtis region show variability in orientation distributions; however, the orientation-frequency distribution in Nili Fossae is preserved in spatial subsets throughout the region (not shown).

3.2. Host Rock

[9] A key result is that ridges are exposed strictly within an altered basement unit that commonly shows strong absorptions in visible/near-infrared reflectance data consistent with the presence of an Fe/Mg-rich smectite clay [*Mangold et al.*, 2007; *Mustard et al.*, 2007, 2009]. Although high spatial resolution spectral data are geographically limited, there is enough coverage to confirm that this is a robust result, and in many cases, morphologic properties of the clay-bearing unit (paucity of impact craters, albedo, and brecciated) allows identification outside of spectrally covered areas. The erosionally recessive clay-bearing basement is the deepest exposed bedrock unit in both mapping regions. In both the Nili Fossae and Nilosyrtis regions, ridges are stratigraphically confined to the clay-bearing basement unit and their exposure consistently terminates at the contact with an overlying variably altered mafic to ultramafic ridge-free cap rock [e.g., *Mustard et al.*, 2007].

4. Discussion

4.1. Nilosyrtis

[10] The spread in ridge orientation values is a manifestation of the irregular branching patterns observed on the crater floors where variably oriented ridges intersect, occasionally appearing to offset other ridges. If the ridges are related to predominately opening-mode fractures in the crust rather than to a depositional origin, then the orientation distributions reflect the state of stress in the crust at the time of fracturing. Qualitatively, HiRISE DEMs suggest that ridges are nearly vertically dipping such that their orientation in the long dimension would be perpendicular to the map direction of maximum extension at the time of formation. Variability of ridge orientations could be a result of multiple generations of fracturing with changing stress fields or local stress heterogeneity related to lithology or preexisting fractures and weaknesses. Despite being spatially separated by <100 km, orientations from three craters in Nilosyrtis show marked differences in ridge orientation-frequency maxima as well as orientation distribution patterns, which suggest that local rather than regional stresses dominated fracture orientations. Ridge orientations may preserve a record of the stress state that evolved during each individual impact event and subsequent crustal adjustment.

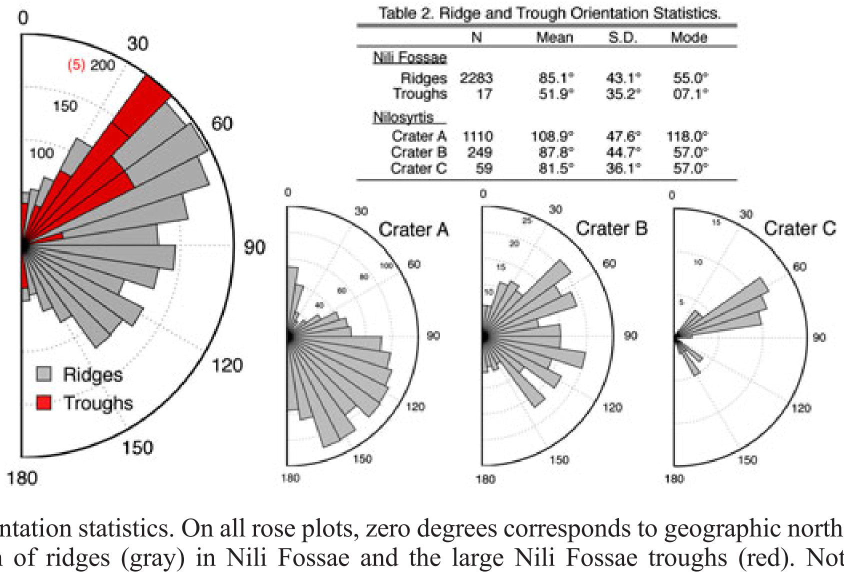

Table 2. Ridge and Trough Orientation Statistics.

	N	Mean	S.D.	Mode
Nili Fossae				
Ridges	2283	85.1°	43.1°	55.0°
Troughs	17	51.9°	35.2°	07.1°
Nilosyrtis				
Crater A	1110	108.9°	47.6°	118.0°
Crater B	249	87.8°	44.7°	57.0°
Crater C	59	81.5°	36.1°	57.0°

Figure 3. Ridge orientation statistics. On all rose plots, zero degrees corresponds to geographic north. (far left) Orientation-frequency distribution of ridges (gray) in Nili Fossae and the large Nili Fossae troughs (red). Note the frequency-scale difference between ridges (n = 2283) and troughs (n = 17). (bottom right) Orientation-frequency distributions of three impact craters in the Nilosyrtis region. (top right) Table of ridge orientation statistics for each rose plot.

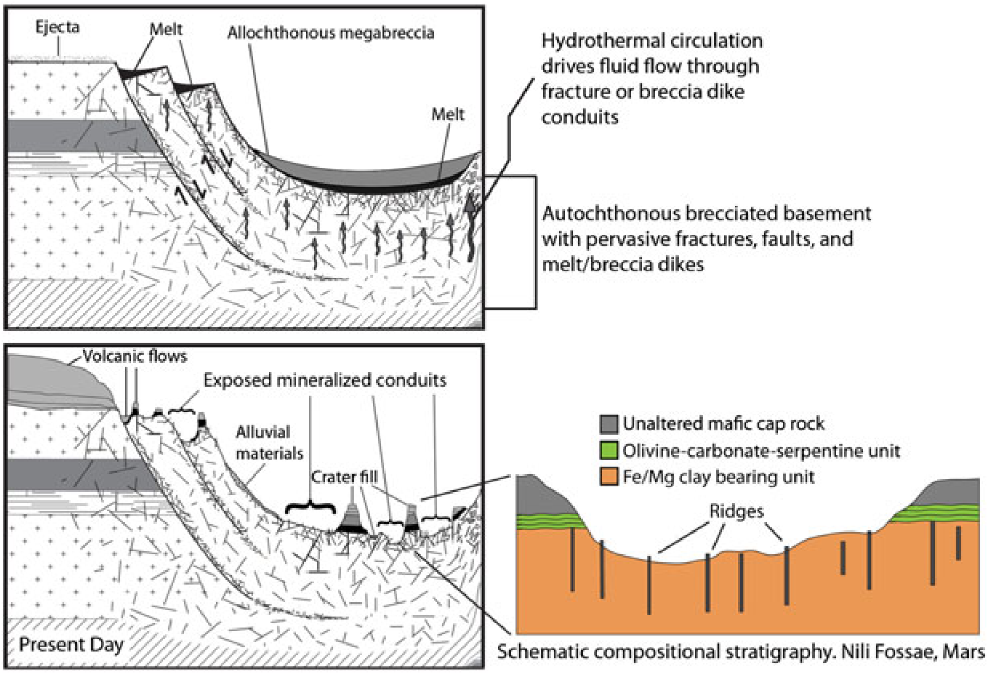

Figure 4. Schematic diagram showing elements of the proposed sequence of events that led to ridge expression. (top) Setting in geologic past in the aftermath of an impact sequence and before external modification processes (i.e., external crater fill and fluvial erosion). (bottom) Present-day surface and subsurface, after crater filling, burial, and incision, exposing cemented impact-related deformation features. (bottom right) Representative cross-section showing the stratigraphy from the Nili Fossae.

4.2. Nili Fossae

[11] Within the broad range of orientation values represented in the Nili Fossae, there is a population of ridge orientations concentrated at ~55° azimuth that may correspond to a weak but present preferred orientation (mode = 55.0°, mean = 85.1°, standard deviation = 39°). This orientation-frequency maximum does not appear to depend on ridge length nor on location within the study area. The average measured orientation of Nili Fossae troughs is 51.9° and trough orientations plotted in red over the ridge orientations for comparison (Figure 3). Qualitatively, the orientation-frequency maxima of ridges and troughs concentrate around the same value, although the sample size for the troughs (n = 17) is small. The ridge and trough orientations have important implications for the stress environment during the emplacement of ridge-precursor structures as well as constraints on the timing and mechanism of the formation of ridges.

4.3. Magmatic Origin

[12] Our quantitative ridge orientation data sets suggest that the ridge networks do not represent the expression of exhumed intrusive magmatic dikes. As observed in terrestrial examples as well as on Mars [*Head et al.*, 2006; *Korteniemi et al.*, 2010; *Pedersen et al.*, 2010], exhumed magmatic dikes typically form broad linear to curvilinear ridges rather than dense intersecting networks. Both on Earth and in proposed Martian examples, swarms of dikes often have roughly unimodal orientation distributions with ridges occurring in parallel to subparallel clusters that extend over several to hundreds of kilometers or in an organization that is concentric and radial to a volcanic source. Ridges in Nili Fossae and Nilosyrtis are oriented over a broad distribution of values that do not correspond to a volcanic center such as Syrtis Major, with the spread of orientations occurring in intervals of >90°, a distribution that is distinctly atypical of magmatic dikes. Magmatic intrusions can produce hardened linear features and if the ridges represent feeder dikes to the resistant cap rock, a magmatic composition could plausibly account for the hardness difference between ridges and the altered host rock. However, the correlation of exposures of dense ridge networks to eroded crater floors and rims over a broad region would implicate a spatially extensive and diffuse magma source that has not been supported by surface observations or anomalies in gravity data.

4.4. Origin of Ridge Networks

[13] Based on these observations, we propose that networks of linear ridges in Nili Fossae represent the erosional expression of permeable complexes that were hardened relative to the host rock (Figure 4). The fossil conduits were impact-related fractures, faults, or breccia-melt–bearing dikes that were formed by brittle failure or clastic intrusion. The fluids necessary to cement these fractures may have been sourced from the hydrous clays pervasive in the host rock, dehydrated from an elevated geotherm upon burial or from impact hydrothermalism. Alternatively, pore fluids may have flowed into fractures, faults, and permeable intrusions, driven by a thermal gradient along the path of least resistance. Clay dehydration may have also helped to facilitate tensile failure in the host rock, especially at low confining pressure, and could have also triggered the emplacement of fluidized clastic or breccia intrusions [*Davies et al.*, 2006]. Other hardening mechanisms cannot be excluded, including intrusion of resistant material, and the ridge networks likely represent a complex of resistant features that have been variably indurated by mineralization. The interpretations from Nili Fossae are consistent with

observations in the Nilosyrtis highlands where a similar stratigraphy and a set of morphologies are observed [*Head and Mustard*, 2006]. The proposed fossilized zones of concentrated fluid flow may represent preserved elements of regional subsurface hydrologic activity that could have been a viable and persistent habitable zone.

4.5. Relative Timing of Events in Nili Fossae

[14] The distribution of ridge orientations in Nili Fossae (n = 2283) show a preferred orientation that aligns with the long dimension of the Nili Fossae graben. The grabens are interpreted to have formed due to flexure and extension of the crust from loading of the Isidis Basin after the impact event [*Wichman and Shultz*, 1989] and the formation of ridge-precursor structures may be associated with the same deformation event. The Nili Fossae grabens have been used as a major stratigraphic marker for interpreting crosscutting relationships in the region and the ridges, which are restricted to the basement unit, may aid in interpreting the relative timing of emplacement of key geologic units. For example, the ridges terminate exposure at the contact of the clay-bearing basement and an overlying cap rock unit, which is crosscut by the graben. The stratigraphic confinement of ridges may be related to the rheological differences between the two units during the formation of ridge-precursor structures, differences in water availability in the units to seal the fluid conduits (clay-bearing versus a dry unit), or could be related to the relative timing of the formation of ridges and emplacement of the overlying unit.

5. Implications for Martian Hydrology

[15] Formation of ridge-precursor structures and their subsequent mineralization may be prevalent on Mars, particularly during its early history when impactor sizes and impact rates were the highest and potentially more of the hydrated crust was exposed at the surface or near-surface as impact target materials. We find evidence of ridge exposure in more or less every degraded crater in the study regions and morphologically similar ridge complexes occur elsewhere on Mars, including in Arabia Terra, northern Meridiani Planum, Solis Planum, Noachis Terra, Atlantis Chaos, and Nepenthes Mensa. We do not observe any linear ridges in craters that appear to postdate regional gradational activity, although they excavate and expose crust at elevations comparable with nearby ridge exposures, which suggests that ridges formed either in Noachian-aged basement or in sedimentary crater fill. In all cases, the ridges are confined to eroded terrains that expose altered crust and are observed to terminate at the contact with an overlying cap unit. This coarse stratigraphy may be representative of impact craters on Mars, particularly those whose cavity floor coincides with the altered ancient megaregolith. If this stratigraphy and the occurrence of fracture networks are ubiquitous in ancient terrains, then impact-induced fracture, faulting, and clastic intrusion may have been a major driver in establishing the local to regional-scale permeability structure of the crust. We propose that these observations substantiate the claim that the early crust of Mars was hydrothermally active and that the interaction between impact heat transfer, deformation, and a preexisting altered basement may have facilitated large-scale interconnected hydrologic networks and widespread alteration [*Ehlmann et al.*, 2011].

[16] **Acknowledgments.** This work was partially supported by a grant from the NASA Rhode Island Space Grant Consortium to Lee M. Saper and by NASA through a subcontract with the Applied Physics Lab at Johns Hopkins University to John F. Mustard.

References

Davies, R. J., M. Huuse, P. Hirst, J. Cartwright, and Y. Yang (2006), Giant clastic intrusions primed by silica diagenesis, *Geology*, *34*, 917–920.

Ehlmann, B. L., et al. (2009), Identification of hydrated silicate minerals on Mars using MRO-CRISM: Geologic context near Nili Fossae and implications for aqueous alteration, *J. Geophys. Res.*, *114*, doi:10.1029/2009JE003339.

Ehlmann, B. L., J. F. Mustard, S. L. Murchie, J.-P. Bibring, A. Meunier, A. A. Fraeman, and Y. Langevin (2011), Subsurface water and clay mineral formation during the early history of Mars, *Nature*, *479*, 53–60.

Ivanov, M. A., H. Hiesinger, G. Erkeling, F. J. Hielscher, and D. Reiss (2012), Major episodes of geologic history of Isidis Planitia on Mars, *Icarus*, *218*, 24–46.

Head, J. W., and J. F. Mustard (2006), Breccia dikes and crater-related faults in impact craters on Mars: Erosion and exposure on the floor of a crater 75 km in diameter at the dichotomy boundary, *Meteorit. Planet. Sci.*, *41*, 1675–1690.

Head, J. W., L. Wilson, J. Dickson, and G. Neukum (2006), The Huygens-Hellas Giant Dike System on Mars: Implications for Late Noachian–Early Hesperian Volcanic Resurfacing and Climatic Evolution, *Geology*, *34*, 285–288.

Korteniemi, J., J. Raitala, M. Aittola, M. A. Ivanov, V.-P. Kostama, T. Öhman, and H. Hiesinger (2010), Dike indicators in the Hadriaca Patera–Promethei Terra region, Mars, *Earth Planet. Sci. Lett.*, *294*, 466–478.

Malin, M. C., et al. (2007), Context Camera Investigation on board the Mars Reconnaissance Orbiter, *J. Geophys. Res.*, *112*, doi:10.1029/2006JE002808.

Mangold, N., et al. (2007), Mineralogy of the Nili Fossae region with OMEGA/Mars Express data: 2. Aqueous alteration of the crust, *J. Geophys. Res.*, *112*, doi:10.1029/2006JE002835.

McEwen, A. S., et al. (2007), Mars Reconnaissance Orbiter's High Resolution Imaging Science Experiment (HiRISE), *J. Geophys. Res.*, *112*, doi:10.1029/2005JE002605.

Mustard, J. F., F. Poulet, J. W. Head, N. Mangold, J.-P. Bibring, S. M. Pelkey, C. I. Fassett, Y. Langevin, and G. Neukum (2007), Mineralogy of the Nili Fossae region with OMEGA/Mars Express data: 1. Ancient impact melt in the Isidis Basin and implications for the transition from the Noachian to Hesperian, *J. Geophys. Res.*, *112*.

Mustard, J. F., B. L. Ehlmann, S. L. Murchie, F. Poulet, N. Mangold, J. W. Head, J.-P. Bibring, and L. H. Roach (2009), Composition, Morphology, and Stratigraphy of Noachian Crust around the Isidis Basin, *J. Geophys. Res.*, *114*, doi:10.1029/2009JE003349.

Okubo, C. H., and A. S. McEwen (2007), Fracture-controlled paleo-fluid flow in Candor Chasma, Mars, *Science*, *315*(5814), 983–985.

Pedersen, G. B. M., J. W. Head, III, and L. Wilson (2010), Formation, erosion and exposure of Early Amazonian dikes, dike swarms and possible subglacial eruptions in the Elysium Rise/Utopia Basin Region, Mars, *Earth Planet. Sci. Lett.*, *294*, 424–439.

Squyres, S. W., et al. (2012), Ancient impact and aqueous processes at Endeavor Crater, Mars, *Science*, *336*(6081), 570–576.

Tornabene, L. L., J. E. Moersch, H. Y. McSween, V. E. Hamilton, J. L. Piatek, and P. R. Christensen (2008), Surface and crater-exposed lithologic units of the Isidis Basin as mapped by coanalysis of THEMIS and TES derived data products, *J. Geophys. Res.*, *113*, doi:10.1029/2007JE002988.

Wichman, R. W., and P. H. Schultz (1989), Sequence and Mechanisms of Deformation Around the Hellas and Isidis Impact Basins on Mars, *J. Geophys. Res.*, *94*, 17333–17357.